nature biotechnology

Dynamic regulation of metabolic flux in engineered bacteria using a pathway-independent quorum-sensing circuit

Apoorv Gupta[1,2], Irene M Brockman Reizman[3,4], Christopher R Reisch[3,4] & Kristala L J Prather[2,3]

Metabolic engineering of microorganisms to produce desirable products on an industrial scale can result in unbalanced cellular metabolic networks that reduce productivity and yield. Metabolic fluxes can be rebalanced using dynamic pathway regulation, but few broadly applicable tools are available to achieve this. We present a pathway-independent genetic control module that can be used to dynamically regulate the expression of target genes. We apply our module to identify the optimal point to redirect glycolytic flux into heterologous engineered pathways in *Escherichia coli*, resulting in titers of *myo*-inositol increased 5.5-fold and titers of glucaric acid increased from unmeasurable to >0.8 g/L, compared to the parent strains lacking dynamic flux control. Scaled-up production of these strains in benchtop bioreactors resulted in almost ten- and fivefold increases in specific titers of *myo*-inositol and glucaric acid, respectively. We also used our module to control flux into aromatic amino acid biosynthesis to increase titers of shikimate in *E. coli* from unmeasurable to >100 mg/L.

Metabolic engineering manipulates the cellular metabolism of microbes to maximize production of value-added products. Heterologous pathways compete with cellular metabolism, thus limiting product yields and affecting cell growth. Several approaches have been used to optimize steady-state flux distributions[1,2]; however, traditional strategies such as gene knockouts, expression level tuning and protein engineering cannot address challenges associated with more complex pathways and products[3] for which it may be necessary to modify metabolic behavior during the course of a production run. Examples of such challenges include pathways that interfere with host metabolism by depleting essential metabolite pools[4], have branchpoints with promiscuous enzymes[5] or synthesize toxic intermediates or products[6]. In such cases, it may prove advantageous to downregulate competing essential pathways or delay expression of engineered pathway enzymes until midway through the cultivation. Such flux control may allow substrate pools to accumulate and then be siphoned into the engineered pathway, analogous to the "just-in-time transcription" that is prevalent in natural systems[7].

Engineered strains that can self-regulate and redirect pathway fluxes could maximize microbial yields and minimize the need for human supervision of fermentations. Several genetic circuits for dynamic pathway regulation have been designed, for example, to produce lycopene[8], amorphadiene[9] and lysine[10]. Most of these circuits have pathway-specific parts, such as metabolite-responsive transcription factors or riboswitches, that limit their use in other pathways and hosts. Broadly applicable circuits should be portable across contexts[11] and designed with industry in mind. Moreover, inducers, especially physiologically active small molecules, are prohibited in most bioprocesses because their use adds costs in downstream processing[12,13]. Although semi-autonomous, generalized strategies for dynamic flux regulation have been reported[14,15], no fully autonomous pathway-independent regulation modules have been constructed to systematically evaluate performance improvements and process robustness with consideration for industrial applicability.

Levels of endogenous gene expression especially those for essential pathway genes, are often low and tightly regulated, such that any perturbation of protein levels that results from swapping native and heterologous parts to institute dynamic control may not be tolerated by a host cell[16–18]. Thus, genetic circuits targeting such genes must enable precise tunability of expression and impose a minimal metabolic burden on the cell. To create a pathway-independent, inducer and intervention-free genetic device to dynamically control endogenous gene expression without imposing a metabolic burden on the host, we turned to quorum-sensing circuitry.

Quorum sensing (QS) functions to control cell-density-dependent processes in bacteria, and has been applied for induction of recombinant protein expression[15], control of lysis[19] and balancing of multiple cell populations[20]. Specific small-molecule signals accumulate in cell populations and induce activation of QS circuits and expression of the genes that they control. We used parts of the Esa QS system from *Pantoea stewartii*[21] to create circuit variants that switch off gene expression at desired times and cell densities. Integration of these circuits into the *E. coli* genome enabled dynamic control of endogenous essential genes in glycolysis and the biosynthesis of aromatic amino acids, which compete with bioproduction of glucaric acid and shikimic acid, respectively. We applied our QS-based circuit to restrict flux through endogenous pathways and siphon carbon substrate into the desired product. Following this, increases in production of *myo*-inositol

[1]Department of Biological Engineering, Massachusetts Institute of Technology, Cambridge, Massachusetts, USA. [2]Synthetic Biology Engineering Research Center (SynBERC), Massachusetts Institute of Technology, Cambridge, Massachusetts, USA. [3]Department of Chemical Engineering, Massachusetts Institute of Technology, Cambridge, Massachusetts, USA. [4]Present addresses: Department of Chemical Engineering, Rose-Hulman Institute of Technology, Terre Haute, Indiana, USA (I.M.B.R.); Department of Microbiology and Cell Science, Institute of Food and Agricultural Sciences, University of Florida, Gainesville, Florida, USA (C.R.R.). Correspondence should be addressed to K.L.J.P. (kljp@mit.edu).

Received 31 August 2016; accepted 13 January 2017; published online 13 February 2017; doi:10.1038/nbt.3796

and glucaric acid of up to 5.5-fold and fourfold, respectively, were achieved, and titers of shikimic acid improved from unmeasurable quantities up to >100 mg/L compared to strains with no dynamic flux control.

RESULTS

Characterization of QS-based autonomous induction

The transcriptional regulator EsaRI70V binds the P_{esaS} promoter in the absence of 3-oxohexanoylhomoserine lactone (AHL)[21] and activates transcription (**Fig. 1a**). Accumulation of AHL occurs as it is produced by the AHL synthase, EsaI, which eventually leads to disruption of EsaRI70V binding and deactivation of the P_{esaS} promoter. By varying the expression level of EsaI, which results in a change of the AHL accumulation rate, we created a library of circuit variants to trigger downregulation of the P_{esaS} promoter at variable times and cell densities over the course of a fermentation. Pre-characterized promoter and ribosome binding sites (RBS) from Mutalik *et al.*[22] were combinatorially assembled to scan a large expression space and achieve a spectrum of EsaI expression levels (**Supplementary Table 1**). Such tuning capabilities permit the discovery and implementation of optimal pathway-specific switching times to modulate flux between endogenous and engineered pathways.

This system can be used to dynamically downregulate the expression of any gene of interest by placing that gene downstream of the P_{esaS} promoter. Degradation tags were added at the C termini of target peptides to ensure that transcribed proteins had short half-lives. The degradation tag provides an additional control mechanism for modulating protein pools and pathway fluxes in the cell. To characterize circuit behaviors and relative switching times, the *esaRI70V* gene was inserted in the genome of *E. coli* MG1655 under the control of a constitutive promoter from the BioFAB library (apFAB104)[23], yielding strain AG2681. *esaI* was subsequently integrated into a combinatorial library of promoter and RBS variants to produce a 28-strain series (called "LXX" in **Supplementary Table 2**) with a range of AHL production rates. A P_{esaS} promoter driving green fluorescent protein (GFP) expression on a medium-copy plasmid (pCOLA-P_{esaS}-GFP(LVA)) was then introduced into the LXX-strain series, (**Supplementary Table 3**), yielding a range of rates at which GFP is switched off. Our attempts to use genomically integrated GFP driven by P_{esaS} resulted in inadequate fluorescence for characterization studies. However, for subsequent pathway-relevant targets in this study, all parts of the circuit, including the P_{esaS} promoter driving the gene of interest, were genomically integrated.

Continuous fluorescence measurements of the LXX-strain series produced a variety of switching times (**Fig. 1b**,**c**). Strain AG2681 had the highest peak fluorescence, as GFP was constitutively expressed due to the absence of EsaI and AHL production. When this strain neared stationary phase and protein production attenuated naturally,

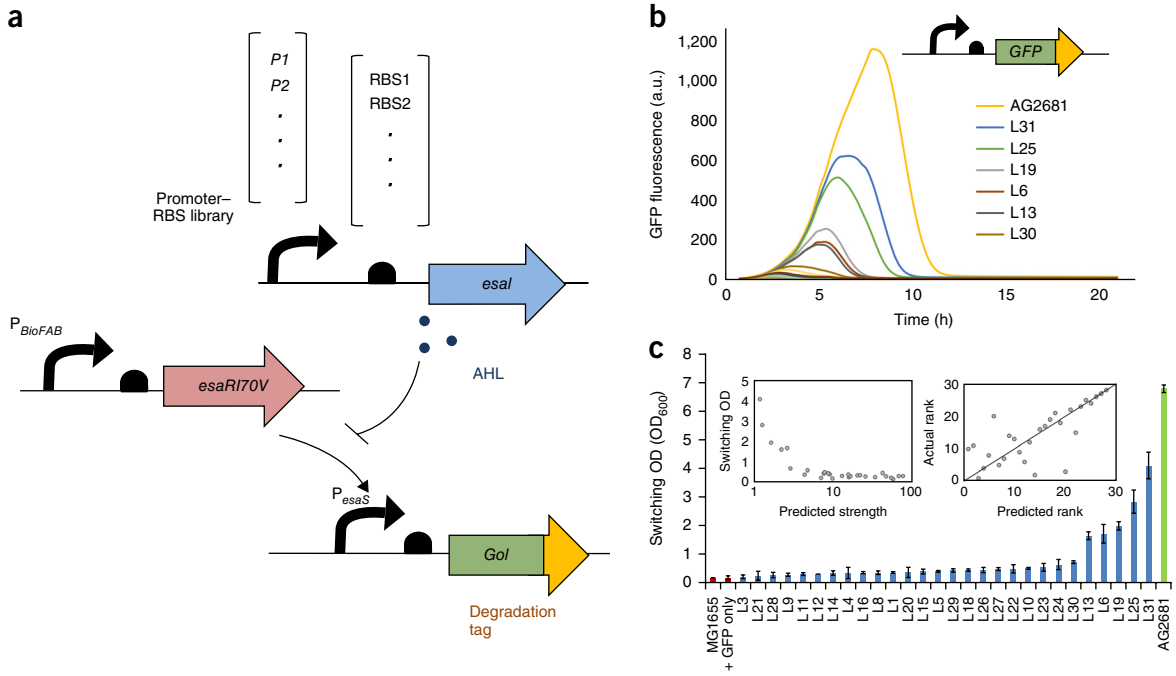

Figure 1 Characterization of a QS circuit to dynamically modulate a target gene of interest (GOI). (**a**) Schematic of the engineered circuit containing a library of promoter–RBS combinations to vary both EsaI expression and AHL production rate and differentially trigger downregulation of any GOI. Stronger EsaI expression leads to earlier downregulation of the GOI. QS-circuit components (*esaI, esaR170V*) are integrated in the genome. All promoter–RBS combinations used to drive *esaI* are described in **Supplementary Table 1**. (**b**) Representative fluorescence profiles for all strains containing GFP under control of the QS circuit. Both switching time and rate vary among strains containing different EsaI expression cassettes. GFP is carried on a medium-copy plasmid to elicit sufficient fluorescence for detection. Fluorescence profiles for all 31 strains tested are depicted, with strain numbers indicated for clearly distinguishable profiles. (**c**) Switching OD for all strains containing GFP under the control of the QS circuit. Constitutive GFP expression in the absence of EsaI (AG2681, green bar), basal expression of GFP in the wild-type MG1655 host without the QS circuit (+ GFP, right red bar) and wild-type MG1655 alone (MG1655, left red bar) were also tested. Switching OD for all strains was plotted against predicted strength of the corresponding promoter–RBS combination driving *esaI*, which was obtained from Mutalik *et al.*[22] (**Supplementary Table 1**) (left inset). All strains with corresponding EsaI cassettes were also rank-ordered based on the measured switching OD (actual rank, early to late switching) and were compared to their corresponding place in the rank-ordered list of switching times based on predicted EsaI strengths from ref. 22 (predicted rank, high to low expression) (right inset). The ranks predicted from switching OD correlated well with the previously predicted ranks, with less agreement at lower ranks (higher EsaI strengths, earlier switching times). Error bars indicate s.d. of triplicate cultures.

the inclusion of the degradation tag led to a decay profile similar to that seen in strains producing AHL. To compare switching rates in the various strains, the cell density corresponding to the time of maximum GFP fluorescence was determined and denoted as the "switching OD." Generally, as the predicted strength of promoter–RBS combinations[22] driving *esaI* increased, peak GFP fluorescence and switching OD decreased. To confirm the consistency of switching times with the predicted order of expression strength, strains were rank-ordered based on their observed switching times and compared with the predicted order of strength of the various EsaI cassettes (**Fig. 1c** insets). Surprisingly, circuit switching seemed highly sensitive to EsaI expression, such that most promoter–RBS combinations led to very low peak GFP and switching ODs (**Fig. 1c**). Only the weakest predicted combinations showed notable delays in GFP knockdown. This indicates that very low levels of EsaI and AHL production are needed for this system to switch, even when the gene encoding the synthase is placed in the genome. The relative trends of switching times observed through GFP characterization matched well with the previously reported order, indicating consistency and reliability in the performance of our circuit and its constituent parts.

Dynamic gene modulation to control glycolytic flux

Given the LXX series of characterized circuit variants, we applied this module to control fluxes in relevant bioproduction pathways. In engineered *E. coli*, a useful node for controlling fluxes in primary metabolism is the metabolic branchpoint at glucose-6-phosphate (G6P, **Fig. 2a**). G6P can be routed into native metabolism through both glycolysis and the oxidative pentose phosphate pathway (PPP), as well as into heterologous production of *myo*-inositol (MI) via *myo*-inositol-1-phosphate synthase (INO1) from *Saccharomyces cerevisiae*[24]. MI can be further converted into other useful products, such as glucaric acid, which is a biopolymer precursor[25], and *scyllo*-inositol, which has been studied as a therapeutic for Alzheimer's disease[26]. The pathway for glucaric acid has been engineered in *E. coli*[4], and theoretical yields of almost 100% are possible; however, G6P is directed into this pathway at the expense of central carbon metabolism. The relative kinetic efficiency between the competing enzymatic branches determines the split of G6P flux in wild-type strains, as well as the potential improvement in MI and glucaric acid titers with dynamic downregulation of native metabolic flux. A mathematical model was built using published *in vitro* kinetic data and information on AHL production dynamics to simulate a QS-based autonomous valve that downregulates glycolytic flux during fermentation (**Supplementary Note 1** and **Supplementary Table 4**).

As phosphofructokinase-1 (Pfk-1; corresponding gene locus denoted *pfkA*) was previously validated as an effective flux control point in upper glycolysis[17], it was chosen as the target gene for dynamic downregulation. A balance between the length of the 'growth mode' (high Pfk-1 activity and glycolytic flux) and 'production mode' (low Pfk-1 activity and glycolytic flux) is predicted to boost MI titers in a defined medium with glucose as the sole carbon source (**Supplementary Fig. 1**). If knockdown in Pfk-1 activity occurs too fast owing to rapid AHL production, titers are suboptimal because growth arrest occurs too early and biomass levels are too low. On the other hand, if knockdown in Pfk-1 occurs too late, the duration of the 'production' mode is too short to allow high titers to accumulate.

To experimentally implement dynamic transcriptional control of Pfk-1 and control glycolytic flux, *zwf* was deleted to prevent flux into the PPP, thereby restricting G6P flux between glycolysis and MI production. All parts of the circuit were genomically integrated. The native promoter of *pfkA* was replaced with the P_{esaS} promoter

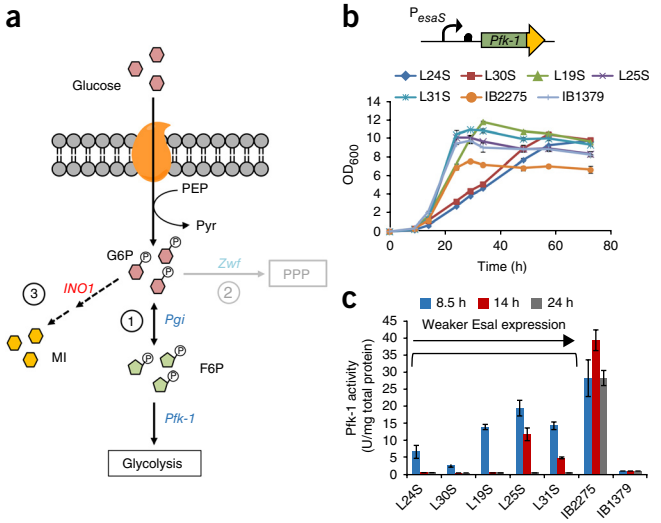

Figure 2 QS-based valve controlling Pfk-1 expression regulates cell growth and flux into central carbon metabolism. All circuit elements are genomically integrated. (**a**) G6P flux is split between three possible branches that include (1) glycolysis, (2) the pentose phosphate pathway (PPP) and (3) MI production through a heterologous pathway. Phosphoglucose isomerase (Pgi) is a reversible enzyme that converts G6P to fructose-6-phosphate (F6P). Pfk-1 catalyzes an irreversible reaction to direct flux further down glycolysis, and it was the gene of interest for dynamic control. Zwf is the entry point into the PPP and is deleted from our strains, while INO1 is the first step toward heterologous formation of MI from G6P. (**b**) Growth profiles show that strains with higher expression of EsaI grow slower. Relative expression strengths for the strains are provided in **Supplementary Tables 1** and **2**. IB2275 does not grow as well and shows a lower final OD_{600}. (**c**) Pfk-1 activity profiles in crude lysates indicate that weaker EsaI expression generally trends with slower decrease in activity over time. IB2275 and IB1379 showed constitutive activity over all time points. EsaI-containing strains displayed high Pfk-1 activities initially, but eventually decreased to below the levels found in IB1379. Data are also provided in tabular format (**Supplementary Table 5**). Error bars denote s.d. of triplicate cultures.

in the native genomic locus, and a standard SsrA degradation tag (AADENYALAA, "LAA") was appended to the C terminus of Pfk-1 to enable rapid removal when transcription has been halted. *esaRI70V* was inserted in the genome under the control of the previously used constitutive promoter (apFAB104)[23], and the final resulting strain was designated IB2275 (**Supplementary Table 2**). This strain constitutively expressed Pfk-1 from P_{esaS} owing to the absence of EsaI and AHL production. In order to allow autonomous downregulation of Pfk-1, *esaI* was inserted in the genome under the control of a subset of the aforementioned expression library (**Supplementary Tables 1** and **2**). Strains were characterized in a minimal medium with glucose as the sole carbon source, thereby coupling Pfk-1 expression and glycolytic flux to cell growth.

A spectrum of growth and Pfk-1 knockdown profiles was obtained (**Fig. 2b**,**c**). With weaker expression of EsaI, the dynamic decay in Pfk-1 activity was slower. As seen in the GFP characterization, however, only the weakest promoter and RBS combinations allowed sufficient delay in AHL accumulation to observe dynamic Pfk-1 knockdown and growth arrest. Promoter–RBS combinations stronger than L24 prevented sufficient growth in the minimal medium because Pfk-1 activity presumably decayed too quickly. Thus, in order to allow enough biomass to build up and to allow switching to occur at an intermediate point in the fermentation, EsaI expression must be low.

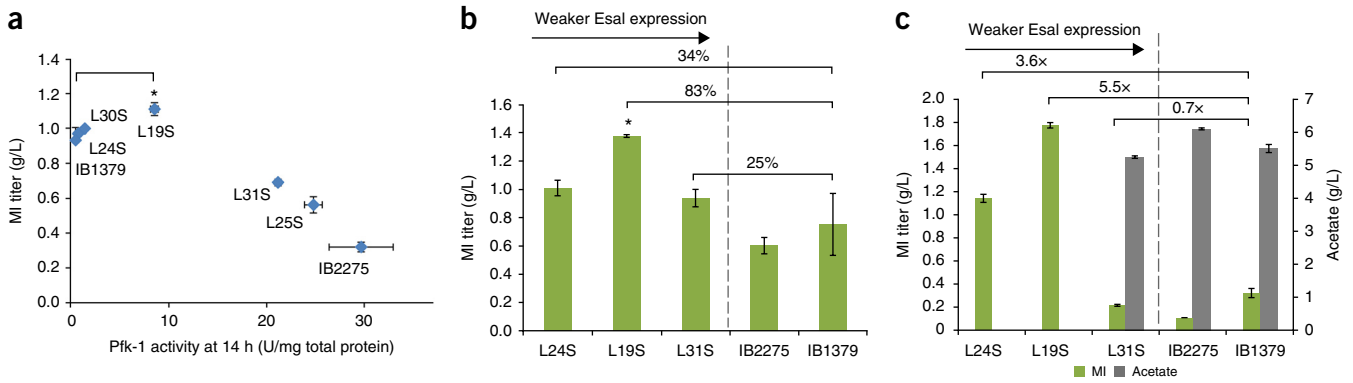

Figure 3 Functionality of QS-based dynamic regulation in multiple culture media. (**a**) MI titers at the endpoint in MOPS minimal medium with 10 g/L glucose plotted against Pfk-1 activity at a given time (14 h post inoculation). An optimum, which yields a 20% titer boost over IB1379, appears that correlates to the most suitable EsaI expression strength (L19S). Corresponding Pfk-1 activity profiles are provided in **Supplementary Figure 3**. (**b**) MI titers from production trials in MOPS minimal medium with 10 g/L glucose and 0.2% casamino acids. Maximum titer was higher than in medium without casamino acids, with a maximum titer boost of 83% for the most productive strain (L19S) over IB1379. Pfk-1 activity profiles are provided in **Supplementary Figure 4a**. (**c**) Endpoint MI and acetate titers in T12 medium containing 10 g/L glucose. Strains that dynamically downregulated Pfk-1 more quickly led to no acetate accumulation and resulted in higher titers (L24S and L19S) with a neutral culture pH. Strains with no dynamic downregulation (IB2275 and IB1379) or a slow decline in Pfk-1 activity (L31S) led to high acetate production, low MI titers and low pH at the end of the batch culture. Pfk-1 activity profiles are provided in **Supplementary Figure 4b**. $*P < 0.05$ relative to titers from IB1379 in a two-tailed *t*-test. Error bars denote s.d. of triplicate cultures.

Switching times in these strains were further elucidated with plasmid-based P_{esaS}–GFP(LVA) using the same analysis procedures as the initial circuit characterization (**Supplementary Fig. 2**). It should be noted that Pfk-1 expression under the control of the P_{esaS} promoter is much higher than from the wild-type promoter, as seen by the differences in activity between IB2275 (P_{esaS} driving *pfkA*) and IB1379 (*pfkA* under its native promoter; **Fig. 2c** and **Supplementary Table 5**). However, when *esaI* is inserted into IB2275, the Pfk-1 activity ultimately drops below the constitutive wild-type level of IB1379. Thus, the P_{esaS} promoter has very strong 'on' and 'off' modes, making it suitable for dynamic pathway flux regulation. The library containing EsaI variants comprises a set of strains to enable switching from 'growth mode' to 'production mode' at different rates in a completely autonomous fashion. The strains can be used to explore trade-offs between yield and titers, thereby allowing the point of maximum productivity to be achieved for any given target product compound branching off from central carbon metabolism.

Optimal strain for *myo*-inositol and glucaric acid production

With successful autonomous control of growth using components of the Esa QS system, the strain series with variable Pfk-1 switching times was applied to improve production of commercially interesting compounds, such as MI and glucaric acid. As described previously, MI branches from glycolysis at the G6P branchpoint and can subsequently be converted to glucaric acid (**Fig. 2a**). For MI production, strains were transformed with pTrc-INO1 (ref. 4) (**Supplementary Table 3**) and tested to determine if switching increases MI titers. Production tests were conducted in MOPS minimal medium supplemented with 10 g/L glucose as the sole carbon source. Not surprisingly, MI production was very poor in IB2275, given its poor growth profile and high Pfk-1 activity (**Supplementary Fig. 3**). However, MI production could be restored to levels equal to or above those in the wild-type IB1379 strain through EsaI expression and control of Pfk-1 activity. Pfk-1 activity profiles for the various EsaI-expressing strains (L24S, L30S, L19S, L25S, L31S) trended consistently with the initial characterization of the GFP library: stronger expression of EsaI led to a faster decline in Pfk-1 activity (**Supplementary Fig. 3**). Further, a boost in MI titers over IB1379 was obtained with an intermediate AHL production rate, as predicted by simulations (**Fig. 3a** and **Supplementary Fig. 1**). Strain L19S exhibited a 20% increase in titer and yield, suggesting that it was able to balance growth and production by decreasing glycolytic flux at a more suitable switching time.

MOPS-based minimal media are used for characterization studies, but scale-up to industrial-scale production will require media formulations tailored to the target pathway and engineered strain. Since previous studies have shown that genetic devices can fail when cultured in a different growth medium[27], we explored the utility of our device in two additional media. In the first case, MOPS-based minimal medium containing 10 g/L glucose was supplemented with 0.2% casamino acids. Pfk-1 activity profiles again showed that stronger expression of EsaI leads to faster activity decline and growth arrest (**Supplementary Fig. 4a**). In addition, measurement of mRNA levels verified that transcriptomic trends were consistent with enzymatic activity data for Pfk-1 (**Supplementary Fig. 5**). MI titers and yields again showed that L19S performed best and led to an 83% improvement over IB1379 (**Fig. 3b**).

We next evaluated strain performance in T12 medium, a phosphate-buffered formulation supplemented with yeast extract and soy peptone that has been developed for industrial bioproduction of glucaric acid[28]. T12 allows faster growth and consumption of glucose, suggesting that it may enable further increases in productivity for a given batch-time compared to MOPS-based minimal medium. Interestingly, in this medium, substantial production of acetate was observed in strains in which Pfk-1 was either constitutively expressed (IB2275 and IB1379) or suppressed too late (L31S) (**Fig. 3c** and **Supplementary Fig. 4b**). Despite the buffering capacity of the medium, the production of excessive acetate owing to overflow metabolism led to a decrease in culture pH (pH ~5.5) and premature growth arrest. Surprisingly, this was also true for the wild-type strain IB1379, in which basal activity of Pfk-1 is considerably lower than in the QS-based IB2275, indicating that even the low levels of wild-type Pfk-1are suboptimal in constitutive mode for product formation branching from glycolysis. On the other hand, strains L19S and L24S were able to suppress Pfk-1 activity earlier, resulting in no acetate surplus

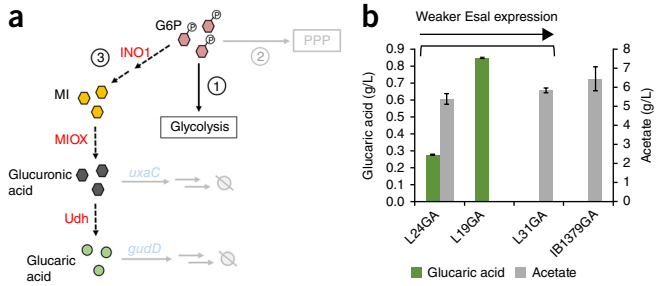

Figure 4 Glucaric acid production using the QS valve at the G6P branchpoint. (**a**) Schematic of the production pathway of glucaric acid from the G6P branchpoint. MI is converted to glucuronic acid by MIOX, which is then converted to glucaric acid by Udh. *uxaC* and *gudD* encode native *E. coli* enzymes that metabolize glucuronic and glucaric acid, respectively; these were deleted to prevent unwanted metabolite consumption. The gene encoding the first step of the pentose phosphate pathway (PPP), *zwf*, was also deleted. (**b**) Glucaric acid and acetate production in strains with varying EsaI expression cassettes. The best producer of glucaric acid is L19GA, which had previously shown the best MI production. With slower (L31GA) or no (IB1379GA) Pfk-1 downregulation, high acetate was detected, but not glucaric acid; this was seen previously with MI production in T12 medium. Error bars denote s.d. of triplicate cultures.

by the end of the fermentation and maintenance of neutral pH. These strains had a significantly higher MI production, with L24S and L19S giving ~3.6-fold and ~5.5-fold boosts, respectively, in endpoint MI titers and yields over IB1379 (**Fig. 3c**). Thus, use of a dynamic strategy was critical to obtain notable titers of MI in a rich medium formulation. MI yields in all cases were proportional to titers as all starting glucose was consumed (**Supplementary Fig. 6**).

Next, glucaric acid production, which requires two further enzymatic steps downstream of MI, was evaluated in the presence of dynamic flux control (**Fig. 4a**). The first step is mediated by *myo*-inositol oxygenase (MIOX) to produce glucuronic acid, which is then followed by uronate dehydrogenase (Udh) to make glucaric acid[4]. Relevant strains (L24GA, L19GA, L31GA and IB1379GA) were prepared from L24S, L19S, L31S and IB1379 by inserting the λDE3 lysogen to allow T7-based expression of pathway enzymes and also by deleting the *uxaC* and *gudD* genes to prevent consumption of glucaric acid or the intermediate—glucuronic acid (**Supplementary Table 2**). Glucaric acid production from glucose has been poor in wild-type K strains, with titers of <0.1 g/L[28,29]. Fermentations were carried out in T12 medium which has been developed for industrial bioproduction of glucaric acid[28]. The IB1379GA control strain with Pfk-1 under the wild-type constitutive promoter showed no detectable production of glucaric acid and instead accumulated acetate (**Fig. 4b**). On the other hand, our most productive engineered strain, L19GA, produced titers up to ~0.85 g/L with minimal acetate accumulation. Similar to MI production in the T12 medium, when Pfk-1 activity was not suppressed early enough or was constitutive (L31GA and IB1379GA), acetate accumulation and low culture pH were observed. In this case, the effect on product titers and yields was even more drastic than during MI production (**Fig. 4b** and **Supplementary Fig. 7**), suggesting that dynamic control is vital.

Scalability for industrial application

Although results from small-scale shake flask cultures were promising, evaluation of our QS-based strategy in more industrially relevant process-development conditions, such as in a stirred-tank bioreactor, is important to justify the potential of this approach for commercial applications[27]. Bioreactors allow for more consistent culture conditions owing to improved mixing and implementation of environmental setpoints such as dissolved oxygen (DO) and pH.

Preliminary trials of MI production in MOPS medium showed the performance in a bench-top bioreactor to be consistent with the initial shake flask results, with a 1.2-fold to twofold increase in titer and yield (**Supplementary Fig. 8**). We also evaluated performance in T12 medium. With implementation of pH control, we hypothesized that despite high acetate production in IB1379, premature growth arrest in the T12 medium could be avoided by controlling culture pH. IB1379 did reach a much higher final OD_{600} than L19S (**Table 1** and **Supplementary Fig. 9**), and there was no residual acetate at the end of the fermentation, presumably because it was reassimilated by the cells. In comparison, L19S reached a lower OD_{600} but yielded an increase of almost tenfold in specific MI titer. We also evaluated glucaric acid production from IB1379GA and L19GA in T12 medium in bioreactors. As seen with MI production trials in bioreactors, there was no residual acetate in IB1379GA fermentations, biomass accumulation was higher than in L19GA fermentations and product titers were low (**Table 1** and **Supplementary Fig. 10**). L19GA produced a nearly fourfold increase in titers over IB1379GA by producing almost 0.7 g/L of glucaric acid (**Table 1** and **Supplementary Fig. 10**).

Production of shikimate using dynamic pathway modulation

In order to test the utility of the Esa QS device in other pathways, we installed this device at a completely different metabolic branchpoint in which dynamic flux regulation is required to improve titers. Shikimate is an intermediate in the chorismate pathway, which eventually leads to the production of aromatic amino acids (AAA)[30] (**Fig. 5a**). It is also a biologically important compound that is an essential starting material for the synthesis of neuraminidase inhibitors, such as Tamiflu, a medication effective in the treatment of influenza[31]. Attempts at bioproduction of shikimate have traditionally involved deleting the genes for shikimate kinases, *aroK* and *aroL*, prohibiting the conversion of shikimate to shikimate-3-phosphate[30]. The fermentation

Table 1 MI and glucaric acid production in T12 medium in a 3-L bioreactor

Strain	Product titer (g/L)	Final OD_{600}	Specific titer (g MI/g DCW)	Yield (g MI/g glucose)
MI production				
IB1379	0.23 ± 0.07	17.4 ± 0.8	0.03 ± 0.01	0.023 ± 0.007
L19S	1.28 ± 0.02	10.2 ± 0.5	0.27 ± 0.01	0.128 ± 0.002
Glucaric acid production				
IB1379GA	0.17 ± 0.02	13.4 ± 0.7	0.03 ± 0.01	0.003 ± 0.001
L19GA	0.68 ± 0.11	10.5 ± 0.8	0.14 ± 0.01	0.014 ± 0.001

QS-based dynamic control of Pfk-1 activity boosted specific titers of MI by almost tenfold and of glucaric acid by almost fivefold, indicating that the QS device functions consistently across shake flasks and bioreactor scales. With QS-based Pfk-1 downregulation, cultures reached a lower biomass and gave higher titers of product, presumably owing to the redirection of flux from central carbon metabolism into heterologous production. Culture growth profiles are provided in **Supplementary Figures 9** and **10**. DCW refers to the dry cell weight in the culture at the endpoint. Error is represented as s.d. of duplicate bioreactor runs.

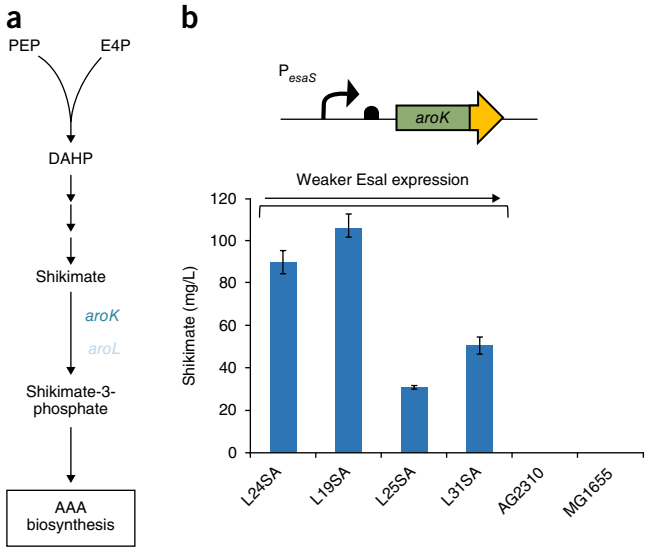

Figure 5 Shikimate production through the aromatic amino acid (AAA) biosynthesis pathway using the QS valve. (**a**) Shikimate is an intermediate in the AAA biosynthesis pathway, whose accumulation competes with production of the AAA. To enable accumulation of shikimate without supplementing with costly AAA, AroK was dynamically downregulated using the QS valve. Native copies of *aroK* and *aroL*, the isozymes of shikimate kinase, were deleted. (**b**) Shikimate titers in strains with various EsaI expression cassettes. With constitutive AroK expression, as in wild-type MG1655 or in a QS strain lacking EsaI (AG2310), there is no accumulation of shikimate. With differential EsaI expression, an optimal strain emerges that maximizes the production of shikimate to >100 mg/L. Error bars denote s.d. of triplicate cultures.

medium must consequently be supplemented with expensive AAA to facilitate growth[30]. Recent academic studies and patent literature have suggested that dynamically downregulating AroK and AroL can mitigate the need for such supplementation, as AAA can be synthesized in the first phase of the fermentation to allow growth, which is then followed by shikimate accumulation[32,33]. Unlike the G6P branchpoint, for which endogenous flux was siphoned into a heterologous pathway for glucaric acid production, this case requires the accumulation of an endogenous metabolite and thereby presents an alternative scenario for the relevance of autonomous, dynamic pathway modulation.

To test our hypothesis, we used our device to dynamically control AroK expression. *aroL* was deleted, while a weak SsrA degradation tag (AANDENYAASV, "ASV") was added to *aroK* and placed under the P_{esaS} promoter in the wild-type MG1655 genome. *esaRI70V* was also driven from a constitutive promoter (apFAB104)[23] in the genome, resulting in strain AG2310 (**Supplementary Table 2**). It is important to note that initial attempts to add stronger SsrA degradation tags to genomic *aroK* prevented the strain from growing in MOPS minimal medium without AAA supplementation, again demonstrating the sensitivity of cell viability to changes in endogenous gene expression. In order to implement dynamic downregulation of AroK, selected weak cassettes from the EsaI expression library were inserted in strain AG2310, which led to a set of strains with different switching times (L24SA, L19SA, L25SA and L31SA; **Supplementary Table 2**). Cultivation in MOPS minimal medium resulted in varied accumulation of shikimate, with an intermediate switching time yielding the highest shikimate accumulation of more than 105 mg/L (**Fig. 5b**). Strain AG2310 and wild-type MG1655 were able to grow in minimal medium without AAA supplementation but were unable to accumulate any shikimate with constitutive AroK expression. To our knowledge, this is the first demonstration of shikimate accumulation in defined minimal medium without addition of AAA, validating our Esa QS device as a generalizable tool for dynamic pathway modulation.

DISCUSSION

We report the engineering of tunable genetic circuits using parts from a bacterial QS system to exercise autonomous, dynamic control over target metabolic genes and to redirect pathway fluxes. These circuits were built from pathway-independent parts, and were applied to regulate metabolic fluxes and achieve substantial increases in titers of various products. Previous studies of dynamic regulation have proposed strategies to sense and respond to specific intermediates[34,35], cell states[9] or medium compositions[36]. Although these strategies can be effective, they are specific to the pathway for which they are developed. Using nutrient starvation is a well-established regulatory control strategy[36], but our attempts to boost MI titers with a circuit that responds to phosphate depletion suggested that nutrient perturbations result in global metabolic effects that are unknown, thus limiting widespread use (**Supplementary Note 2**, **Supplementary Fig. 11**).

As endogenous gene expression is often low and highly regulated, tight control during both 'on' and 'off' states is required. Transcription of the target gene can be abrogated by our QS circuit, but cellular protein pools must also be depleted to observe phenotypic changes. We altered natural degradation rates by appending degradation tags to target proteins. Strong tags were required to deplete GFP and Pfk-1 pools, whereas a weaker tag was needed to ensure sufficient AroK levels in the 'on' state. Fluorescence profiles of a subset of strains in **Figure 1c** with untagged GFP confirmed that degradation tags are needed to deplete these stable proteins (**Supplementary Fig. 12**). Precise tunability of a circuit was achieved through a chromosomal library of EsaI expression levels, revealing that circuit switching times were optimal at the lowest EsaI expression levels. This highlights the sensitivity of circuit-triggering time to the production rate of AHL and underscores the fact that endogenous gene expression only needs to be slightly perturbed to substantially affect production of heterologous compounds. Our attempts to use a reverse QS-circuit configuration in which an activating promoter was driving expression of SspB, an SsrA-dependent degradation protein targeted to Pfk-I, failed, as even leaky expression completely suppressed growth (**Supplementary Note 3** and **Supplementary Figs. 13** and **14**).

Our system is tunable and fully autonomous, and does not require addition of an external inducer. A library of EsaI circuits that produce the 'trigger molecule' at variable rates resulted in a series of strains that provide different switching rates, making it possible to find the optimal circuit for any pathway. Despite ample evidence that circuits developed for product synthesis often fail to translate from the laboratory to industry[27], robustness of synthetic biology devices is often overlooked. Quorum sensing relies on extracellular signals which can vary upon mixing[37], so it is vital to scale studies up into bioreactors to prove they are translatable to industrial contexts. We evaluated our QS circuits in various media and found that with richer, industrially-relevant medium, dynamic regulation prevented overflow metabolism and unwanted acetate production. Performance of our circuit in shake flasks and bioreactors was consistent, and revealed how carbon flux in central metabolism can be wasted by excess acetate and biomass production.

Dynamic regulation of pathway fluxes has emerged as a new frontier in metabolic engineering[38–40]. The QS system we have developed enables precise tunability of an engineered pathway with minimal upfront effort in any growth environment. As production strategies become more complex, host genetic backgrounds become more

cumbersome to engineer. The strategies we report here exemplify the next stage in dynamic metabolic engineering, with standardized and streamlined engineering methods.

METHODS

Methods, including statements of data availability and any associated accession codes and references, are available in the online version of the paper.

Note: Any Supplementary Information and Source Data files are available in the online version of the paper.

ACKNOWLEDGMENTS

We thank C. Collins at Rensselaer Polytechnic Institute (Troy, New York, USA) for providing plasmids and parts for the Esa QS system. In addition, we thank S. Arussy for help in preparing strains for glucaric acid production, and m2p-labs for the loan of a BioLector unit. This work was supported by the US National Science Foundation through the CAREER program (I.M.B.R. and K.L.J.P., Grant No. CBET-0954986), the Graduate Research Fellowship program (A.G.), the Synthetic Biology Engineering Research Center (SynBERC; A.G. and K.L.J.P., Grant No. EEC-0540879), and the Division of Molecular and Cellular Biosciences (A.G. and K.L.J.P., Grant No. MCB-1517913); by the Biotechnology Training Program of the National Institutes of Health (I.M.B.R., Grant No. T32GM008334); and by the USDA National Institute of Food and Agriculture Postdoctoral Fellowship (C.R.R., Grant No. 2013-67012-21022).

AUTHOR CONTRIBUTIONS

A.G., I.M.B.R., C.R.R. and K.L.J.P. designed and performed the experiments and analyzed the data. A.G., I.M.B.R. and K.L.J.P. wrote the manuscript.

COMPETING FINANCIAL INTERESTS

The authors declare competing financial interests: details are available in the online version of the paper.

1. Alper, H., Miyaoku, K. & Stephanopoulos, G. Construction of lycopene-overproducing *E. coli* strains by combining systematic and combinatorial gene knockout targets. *Nat. Biotechnol.* **23**, 612–616 (2005).
2. Biggs, B.W., De Paepe, B., Santos, C.N.S., De Mey, M. & Kumaran Ajikumar, P. Multivariate modular metabolic engineering for pathway and strain optimization. *Curr. Opin. Biotechnol.* **29**, 156–162 (2014).
3. Holtz, W.J. & Keasling, J.D. Engineering static and dynamic control of synthetic pathways. *Cell* **140**, 19–23 (2010).
4. Moon, T.S., Yoon, S.-H., Lanza, A.M., Roy-Mayhew, J.D. & Prather, K.L.J. Production of glucaric acid from a synthetic pathway in recombinant *Escherichia coli*. *Appl. Environ. Microbiol.* **75**, 589–595 (2009).
5. Rodrigues, A.L. *et al.* Systems metabolic engineering of *Escherichia coli* for production of the antitumor drugs violacein and deoxyviolacein. *Metab. Eng.* **20**, 29–41 (2013).
6. Martin, V.J.J., Pitera, D.J., Withers, S.T., Newman, J.D. & Keasling, J.D. Engineering a mevalonate pathway in *Escherichia coli* for production of terpenoids. *Nat. Biotechnol.* **21**, 796–802 (2003).
7. Zaslaver, A. *et al.* Just-in-time transcription program in metabolic pathways. *Nat. Genet.* **36**, 486–491 (2004).
8. Farmer, W.R. & Liao, J.C. Improving lycopene production in *Escherichia coli* by engineering metabolic control. *Nat. Biotechnol.* **18**, 533–537 (2000).
9. Dahl, R.H. *et al.* Engineering dynamic pathway regulation using stress-response promoters. *Nat. Biotechnol.* **31**, 1039–1046 (2013).
10. Zhou, L.-B. & Zeng, A.-P. Exploring lysine riboswitch for metabolic flux control and improvement of L-lysine synthesis in Corynebacterium glutamicum. *ACS Synth. Biol.* **4**, 729–734 (2015).
11. Cardinale, S. & Arkin, A.P. Contextualizing context for synthetic biology--identifying causes of failure of synthetic biological systems. *Biotechnol. J.* **7**, 856–866 (2012).
12. Van Dien, S. From the first drop to the first truckload: commercialization of microbial processes for renewable chemicals. *Curr. Opin. Biotechnol.* **24**, 1061–1068 (2013).
13. Weber, W. & Fussenegger, M. Inducible product gene expression technology tailored to bioprocess engineering. *Curr. Opin. Biotechnol.* **18**, 399–410 (2007).
14. Soma, Y. & Hanai, T. Self-induced metabolic state switching by a tunable cell density sensor for microbial isopropanol production. *Metab. Eng.* **30**, 7–15 (2015).
15. Tsao, C.Y., Hooshangi, S., Wu, H.C., Valdes, J.J. & Bentley, W.E. Autonomous induction of recombinant proteins by minimally rewiring native quorum sensing regulon of *E. coli*. *Metab. Eng.* **12**, 291–297 (2010).
16. Solomon, K.V., Moon, T.S., Ma, B., Sanders, T.M. & Prather, K.L.J. Tuning primary metabolism for heterologous pathway productivity. *ACS Synth. Biol.* **2**, 126–135 (2013).
17. Brockman, I.M. & Prather, K.L.J. Dynamic knockdown of *E. coli* central metabolism for redirecting fluxes of primary metabolites. *Metab. Eng.* **28**, 104–113 (2015).
18. Juminaga, D. *et al.* Modular engineering of L-tyrosine production in *Escherichia coli*. *Appl. Environ. Microbiol.* **78**, 89–98 (2012).
19. Saeidi, N. *et al.* Engineering microbes to sense and eradicate Pseudomonas aeruginosa, a human pathogen. *Mol. Syst. Biol.* **7**, 521 (2011).
20. Balagaddé, F.K. *et al.* A synthetic *Escherichia coli* predator-prey ecosystem. *Mol. Syst. Biol.* **4**, 187 (2008).
21. Minogue, T.D., Wehland-von Trebra, M., Bernhard, F. & von Bodman, S.B. The autoregulatory role of EsaR, a quorum-sensing regulator in Pantoea stewartii ssp. stewartii: evidence for a repressor function. *Mol. Microbiol.* **44**, 1625–1635 (2002).
22. Mutalik, V.K. *et al.* Precise and reliable gene expression via standard transcription and translation initiation elements. *Nat. Methods* **10**, 354–360 (2013).
23. BioFAB. Biofab Data Access Client (BioFAB, 2012).
24. Hansen, C.A., Dean, A.B., Draths, K.M. & Frost, J.W. Synthesis of 1,2,3,4-Tetrahydroxybenzene from D-glucose: exploiting myo-Inositol as a precursor to aromatic chemicals. *J. Am. Chem. Soc.* **121**, 3799–3800 (1999).
25. Werpy, T. *et al.* Top value added chemicals from biomass volume I—results of screening for potential candidates from sugars and synthesis gas (US Department of Energy, Washington, DC, 2004).
26. Yamaoka, M., Osawa, S., Morinaga, T., Takenaka, S. & Yoshida, K. A cell factory of *Bacillus subtilis* engineered for the simple bioconversion of myo-inositol to scyllo-inositol, a potential therapeutic agent for Alzheimer's disease. *Microb. Cell Fact.* **10**, 69 (2011).
27. Moser, F. *et al.* Genetic circuit performance under conditions relevant for industrial bioreactors. *ACS Synth. Biol.* **1**, 555–564 (2012).
28. Reizman, I.M.B. *et al.* Improvement of glucaric acid production in *E. coli* via dynamic control of metabolic fluxes. *Metab. Eng. Commun.* **2**, 109–116 (2015).
29. Raman, S., Rogers, J.K., Taylor, N.D. & Church, G.M. Evolution-guided optimization of biosynthetic pathways. *Proc. Natl. Acad. Sci. USA* **111**, 17803–17808 (2014).
30. Draths, K.M., Knop, D.R. & Frost, J.W. Shikimic acid and quinic acid: replacing isolation from plant sources with recombinant microbial biocatalysis. *J. Am. Chem. Soc.* **121**, 1603–1604 (1999).
31. Kim, C.U. *et al.* Influenza neuraminidase inhibitors possessing a novel hydrophobic interaction in the enzyme active site: design, synthesis, and structural analysis of carbocyclic sialic acid analogues with potent anti-influenza activity. *J. Am. Chem. Soc.* **119**, 681–690 (1997).
32. Way, J.C. & Davis, J.H. Methods and molecules for yield improvement involving metabolic engineering. US Patent Application No. 13/322,383 (2010).
33. Chen, K. *et al.* Deletion of the aroK gene is essential for high shikimic acid accumulation through the shikimate pathway in *E. coli*. *Bioresour. Technol.* **119**, 141–147 (2012).
34. Xu, P., Li, L., Zhang, F., Stephanopoulos, G. & Koffas, M. Improving fatty acids production by engineering dynamic pathway regulation and metabolic control. *Proc. Natl. Acad. Sci. USA* **111**, 11299–11304 (2014).
35. Pfleger, B.F., Pitera, D.J., Newman, J.D., Martin, V.J.J. & Keasling, J.D. Microbial sensors for small molecules: development of a mevalonate biosensor. *Metab. Eng.* **9**, 30–38 (2007).
36. Studier, F.W. Protein production by auto-induction in high density shaking cultures. *Protein Expr. Purif.* **41**, 207–234 (2005).
37. Wang, G. *et al.* Integration of microbial kinetics and fluid dynamics toward model-driven scale-up of industrial bioprocesses. *Eng. Life Sci.* **15**, 20–29 (2015).
38. Brockman, I.M. & Prather, K.L.J. Dynamic metabolic engineering: new strategies for developing responsive cell factories. *Biotechnol. J.* **10**, 1360–1369 (2015).
39. Venayak, N., Anesiadis, N., Cluett, W.R. & Mahadevan, R. Engineering metabolism through dynamic control. *Curr. Opin. Biotechnol.* **34**, 142–152 (2015).
40. McNerney, M.P., Watstein, D.M. & Styczynski, M.P. Precision metabolic engineering: the design of responsive, selective, and controllable metabolic systems. *Metab. Eng.* **31**, 123–131 (2015).

ONLINE METHODS

All strains and plasmids used in this study are summarized in **Supplementary Tables 2** and **3**, respectively. Sequences for specific promoter, 5′ UTRs and degradation tags used in the various expression cassettes are provided in **Supplementary Table 6**. For plasmid preparations and genetic manipulations, cells were cultured in Luria-Bertani (LB) broth at either 30 °C or 37 °C. Temperature-sensitive plasmids were cured at 42 °C. Strain IB1379 was previously constructed[17].

Strain construction. *GFP characterization of QS circuit*. For initial characterization of QS-based transcriptional control with varying switching times, the *esaRI70V* expression cassette was integrated into the genome under the control of a synthetic promoter (apFAB104)[23]. *esaRI70V* is a mutant version of the wild-type *esaR* that was previously engineered to respond to concentrations of AHL at a higher threshold than the wild-type protein[41]. Integration was performed via "clonetegration"[42]. The pOSIP-KH backbone and the desired EsaRI70V expression cassette were digested with KpnI and PstI and ligated overnight. The ligation product was used to transform *E. coli* strain MG1655 for integration at the HK022 locus. The phage integration genes and antibiotic resistance cassette were cured with pE-FLP[42], yielding strain AG2681. The EsaI expression library was installed as described below.

The P_{esaS} promoter was amplified from pCS-PesaS-lux[41] and was appended to GFP that was tagged with a modified SsrA tag (AANDENYALVA, "LVA") using overlap extension PCR to yield P_{esaS}-GFP(LVA). This cassette was inserted into the pCOLA Duet Vector using restriction digestion and ligation to yield pCOLA-P_{esaS}-GFP(LVA) (**Supplementary Table 3**). A separate version of this plasmid was also created in which GFP was not appended to any degradation tag, yielding pCOLA-P_{esaS}-GFP (**Supplementary Table 3**).

Dynamic control of Pfk-1. For QS-based transcriptional control of Pfk-1, the *pfkA* locus was amplified from the *E. coli* genome with primers that appended the standard SsrA degradation tag (AADENYALAA, "LAA"). The P_{esaS} promoter was appended to *pfkA* using overlap extension PCR to yield P_{esaS}-pfkA(LAA). This cassette was used to replace the native *pfkA* locus and the corresponding promoter using the "landing pad" method[43]. Briefly, this cassette was cloned into vector pTKIP-neo by restriction digestion and ligation with HindIII and KpnI, yielding pTKIP-P_{esaS}-pfkA(LAA). Lambda-red-mediated recombination was used to introduce the tetracycline resistance marker and "landing pad" sequences into the genome at the *pfkA* locus in IB1379. This strain was transformed with pTKRED and pTKIP-P_{esaS}-pfkA(LAA), and integration was achieved after cleavage of the pTKIP-P_{esaS}-pfkA(LAA) plasmid and subsequent lambda-red-mediated recombination of the P_{esaS}-pfkA(LAA) and kanamycin resistance cassette sequences into the *pfkA* locus. The kanamycin resistance cassette was cured by expression of FLP recombinase from pCP20. Next, the *esaRI70V* was integrated into the genome under control of a synthetic promoter (apFAB104) at the HK022 phage locus using "clonetegration"[42], as described previously, yielding strain IB2275.

Dynamic control of AroK. For QS-based dynamic control of the shikimate pathway, *aroK* was ligated to the P_{esaS} promoter, and this combined piece was ligated to an expression cassette consisting of *esaRI70V* driven by a synthetic promoter (apFAB104). A weak SsrA tag (AANDENYAASV, "ASV") was appended to the C terminus of *aroK*, yielding *esaRI70V*-P_{esaS}-*aroK(ASV)*. This cassette was genomically integrated, using "clonetegration", into the HK022 locus of a MG1655 strain in which the native copies of *aroK* and *aroL* were deleted, yielding strain AG2310.

EsaI expression library. To implement a library of promoter and RBS variants to drive *esaI* expression from the genome, a select number of promoters and RBS variants were chosen whose combinatorial assembly spanned the predicted expression space in Mutalik *et al.*[22]. We chose five promoters and six RBS variants to give a total library size of 30 combinations. A comprehensive list of all combinations that were constructed for the EsaI expression library and the associated expression strengths is provided in **Supplementary Table 1**. A single RBS variant from the BioFAB registry was used as a template for PCR amplification with primers containing the different promoters at the 5′ end, and the variable regions of the RBS variants at the 3′ end. This led to a series of amplicons containing different promoter and RBS variant combinations. The *esaI* locus was amplified from pAC-EsaRI[44] and was appended to the amplicons containing different promoter and RBS variant combinations. The *esaI* locus was amplified from pAC-EsaRI[44] and was appended to the amplicons containing promoters and RBS variants using overlap extension PCR. The combined fragments were cloned into pOSIP-KO[42] using restriction digestion with Kpn1 and Sph1, and AG2681, IB2275 and AG2310 were transformed with the ligated plasmids to yield a library of strains with *esaI* genomically integrated at the 186 phage locus. The complete list of all combinations of EsaI cassettes and the corresponding strain denotations are given in **Supplementary Table 1**.

To prepare strains to make glucaric acid, the λDE3 lysogen was first inserted into strains L24S, L19S, L31S and IB1379 using a λDE3 Lysogenization Kit (Novagen, Darmstadt, Germany). Next, in order to eliminate catabolism of glucaric acid and the pathway intermediate glucuronic acid, *uxaC* and *gudD* were sequentially deleted from these strains via P1 transduction from the Keio collection donor strains[45], yielding strains L24SGA, L19SGA, L31SGA and IB1379GA (**Supplementary Table 2**).

Phosphate-starvation-based control. A list of all strains used in this study and the relevant genotypes are listed in **Supplementary Table 2**. Strains IB1863, IB1624, IB1643 and IB1379 were previously constructed[17]. To engineer strains that induce *sspB* upon phosphate depletion, the P_{phoA} promoter and a synthetic 5′ UTR were appended to *sspB* using an extended 5′ overhang on the PCR primer for amplification of the *sspB* sequence from the *E. coli* genome. Integration of the *sspB* expression cassette into the genome was carried out via "clonetegration"[42]. The pOSIP-CH backbone and the desired *sspB* expression cassette were digested with KpnI and PstI and ligated overnight. The ligation product was used to transform strains IB1624 and IB1643 for integration at the HK022 locus. The phage integration genes and antibiotic resistance cassette were cured with pE-FLP, yielding the strains IB1509 and IB643.

QS-based post-translational control. To construct strains that utilize QS-based induction of *sspB*, an EsaR-responsive expression cassette for *sspB* expression was first constructed. Briefly, *esaR* was amplified from pAC-EsaR[41] using primers that appended the 5′ UTR and a synthetic promoter (apFAB104). Additionally, P_{esaR} was amplified from pCS-P_{esaR}-lux[41], and *sspB* was amplified from the *E. coli* genome. These three pieces were joined together using overlap-extension PCR to create *esaR*-P_{esaR}-*sspB*. The cassette was cloned into pOSIP-CH[42] using restriction digest with PstI and KpnI, and the resultant construct was used to transform IB1643 to allow genomic integration at the HK022 locus. Phage integration genes and the antibiotic resistance marker were cured with pE-FLP as described previously[42] to yield strain IB2265.

To reduce the translation rate of *sspB,* a genomic RBS library with varying levels of predicted translational efficiency, was inserted into the chromosome using methods described in Reisch *et al.*[46]. Briefly, we first generated a library of RBS variants of different strengths by using the RBS calculator[47] and introducing a three base pair degeneracy into the RBS and 5′ UTR of *sspB* in IB2265. An 80-mer oligonucleotide that targeted the lagging strand of the *sspB* RBS (gttaagtaaaagaagcagccaattcattaaagagNNgaaaggatcNatggatttgtcacagcta acaccacgtcgtccct) that contained three nucleotide degeneracies (denoted as "N" in the sequence above) was obtained. The underlined portion in the sequence denotes the original RBS sequence. In addition, a guide RNA sequence was designed to target a 21-base-pair region (ttaaagaggagaaaggatcca) that was adjacent to an NGG sequence in the original RBS sequence to allow Cas9 counterselection against the wild-type genome. Strain IB2265 was first transformed with plasmid pCas9CR to induce Cas9 expression, and then it was transformed again with pKDsgRNA-sspB, which possessed the lambda Red genes in addition to the sgRNA. Induction of the expression of the lambda Red genes was achieved by the addition of 1% arabinose, and then genes were incubated for 15 min and then transformed with the 80-mer. After a two-hour recovery, the cells were plated on anhydrotetracyline-containing medium to induce Cas9 counterselection. Colonies were screened in the BioLector (m2plabs, Baesweiler, Germany) for growth with and without AHL in MOPS minimal medium (described below), and one was chosen for further characterization, yielding strain AG2349.

Culturing and fermentations. *GFP characterization.* Switching times for the various EsaI variants were quantified using the BioLector microbioreactor system (m2p-labs, Baesweiler, Germany). Individual colonies were inoculated in LB medium and grown overnight at 30 °C. Working 1 mL cultures were inoculated from these seeds into BioLector 48-well flower plates and

doi:10.1038/nbt.3796

incubated at 30 °C, 1200 rpm (3 mm orbit) and 80% relative humidity. The plate was sealed with gas-permeable sealing foil (m2p-labs) to reduce evaporation. Cultures were monitored for OD (BioLector Units) and GFP fluorescence over time. To ascertain switching ODs for a given strain, the corresponding cell density at the point of peak fluorescence was obtained from the fluorescence and biomass time curves. It was assumed that higher AHL production rate and stronger EsaI expression led to lower switching ODs. Strains were rank-ordered based on switching ODs and the trends were compared to the rank-ordered list of strains based on predictions from Mutalik *et al.*[22].

Growth-based screening. The RBS libraries generated to tune down the translation rate of *sspB* were screened for growth using the BioLector microbioreactor system (m2p-labs, Baesweiler, Germany). Individual colonies were inoculated in LB medium, grown overnight at 30 °C at 250 rpm, then diluted 1:100 into modified MOPS medium and grown for ~24 h. Working cultures of 1 mL total volume in MOPS medium were inoculated from this seed in a BioLector 48-well flower plate and incubated at 30 °C, 1200 rpm (3 mm orbit), and 80% relative humidity. Each seed culture was used to inoculate two wells in the BioLector plate: one supplemented with 10 μM AHL and one without AHL. The plate was sealed with gas-permeable sealing foil (m2p-labs) to reduce evaporation. Culture OD was monitored over time.

Shake flask fermentations. Initial growth studies and MI production trials were performed in 250-mL baffled shake flasks with 60 mL working volume at 30 °C and 250 rpm in modified MOPS minimal medium containing 10 g/L D-glucose, 3 g/L NH_4Cl, 1 g/L K_2HPO_4, 2 mM $MgSO_4$, 0.1 mM $CaCl_2$, 40 mM MOPS, 4 mM Tricine, 50 mM NaCl, 100 mM Bis-Tris, 134 μM EDTA, 31 μM $FeCl_3$, 6.2 μM $ZnCl_3$, 0.76 μM $CuCl_2$, 0.42 μM $CoCl_2$, 1.62 μM H_3BO_3 and 0.081 μM $MnCl_2$. When noted, the medium was also supplemented with 0.2% casamino acids. For phosphate starvation experiments, the concentration of K_2HPO_4 in the medium was varied from 0.1 to 1 g/L. For strains containing pTrc-INO1, the medium was also supplemented with 100 μg/mL carbenicillin for plasmid maintenance. Strains were initially grown in 3 mL LB medium at 30 °C overnight, and then diluted 1:100 into 5-mL seed cultures of modified MOPS medium (containing 0.2% casamino acids if the subsequent fermentations were also performed with casamino acids) for ~24 h at 30 °C. These were used to inoculate working flask cultures at OD_{600} 0.05. For MI production trials, shake flask cultures were also supplemented with 50 μM β-D-1-thiogalactopyranoside (IPTG) to induce INO1. Flasks were incubated at 30 °C with 250 rpm shaking and 80% humidity. Samples were taken periodically for measurement of enzyme activity, mRNA quantification, and extracellular metabolites. Fermentations were carried out for 72 or 95 hrs, at which point all glucose was consumed.

Shake flask fermentations to measure MI production were also carried out in T12 medium containing 10 g/L D-glucose, 7.5 g/L yeast extract, 7.5 g/L soy peptone, 7 g/L Na_2HPO_4, 3 g/L KH_2PO_4, 0.5 g/L NaCl, 3 g/L $(NH_4)_2SO_4$, 4 mM $MgSO_4$, as well as 100 μg/μL carbenicillin for plasmid maintenance. Overnight 3 mL cultures were started in T12 medium at 30 °C, and then they were diluted 1:100 into fresh 30 mL starters to grow for ~5 h until the exponential phase was achieved. 60 mL working cultures, supplemented with 50 μM IPTG, were then inoculated at OD_{600} 0.05. Flasks were incubated at 30 °C with 250 rpm shaking and 80% humidity. Samples were taken periodically for measurement of enzyme activity and extracellular metabolites. Fermentations were carried out for 64 h, at which point all glucose was consumed.

Glucaric acid production trials were conducted in T12 medium containing 10 g/L glucose as described above. The λDE3 lysogen was inserted into the strains to be tested (noted above), and the resultant strains were transformed with pRSFD-IN-MI and pTrc-Udh (**Supplementary Table 3** The medium was supplemented with 100 μg/mL carbenicillin and 50 μg/mL kanamycin for plasmid maintenance. Overnight cultures and reinoculation were carried out as described above for MI production. 60 mL working cultures, which were supplemented with 100 μM IPTG to induce the glucaric acid pathway enzymes, were inoculated at OD_{600} 0.05, and flasks were incubated at 30 °C with 250 rpm shaking and 80% humidity. Samples were taken periodically to measure extracellular metabolites.

Shikimate production trials were conducted in modified MOPS medium containing 10 g/L glucose as described above. Strains were initially grown overnight in 3 mL LB medium and then diluted 1:100 into 5 mL seed cultures of modified MOPS medium for ~24 h at 30 °C. These were used to inoculate 50 mL working flask cultures at OD 0.05. Flasks were incubated at 30 °C with 250 rpm shaking and 80% humidity. Samples were taken periodically for measurement of extracellular metabolites, and fermentations were carried out for 72 h until all glucose was consumed.

Production trials in bioreactors. Scale-up production trials for MI were carried out in either the modified MOPS minimal medium described previously or T12 medium in a standard 3L benchtop bioreactor (Infors HT, Bottmingen, Switzerland). For MOPS trials, LB cultures inoculated overnight were used to inoculate seed cultures in modified MOPS minimal medium, which were then grown at 30 °C for ~24 h. For trials in T12 medium, cultures were grown overnight in T12 medium at 30 °C. These were diluted 1:100 in fresh T12 medium and allowed to grow for ~5 h until the exponential phase was achieved. In both cases, a 1.25 l working culture, containing 50 μM IPTG to induce INO1, was inoculated to an initial OD_{600} 0.05 for MI production. All cultivations were done in the presence of 100 μg/mL carbenicillin for plasmid maintenance. During fermentation, oxygen was supplied by filtered air at 0.75 l/min and agitation was adjusted to maintain a 35% dissolved oxygen level (250–750 rpm). The pH of the culture was set to 7.0 and controlled by addition of 4 M NaOH. The temperature of the culture was maintained at 30 °C. Samples were taken periodically for measurement of extracellular metabolites and dry cell weight (calculated from measured OD_{600} values as $0.47\times OD_{600}$). Two independent trials were run for each bioreactor experiment.

Glucaric acid production trials in T12 medium were carried out with a protocol similar to that of the MI production trials with the following changes. For maintenance of both plasmids, 100 μg/mL carbenicillin and 50 μg/mL kanamycin were used. Induction of all pathway enzymes was achieved with 100 μM IPTG.

Phosphofructokinase activity assays. Samples for activity assays of Pfk-1 were collected over the course of the fermentations. Activity measurements were carried out according to the protocol reported previously[17].

Quantification of mRNA levels. To quantify the relative transcript levels of *pfkA* across various strains, 1 mL samples were collected over the course of the fermentation and mixed with 2 mL of RNAprotect bacteria reagent (Qiagen). These samples were vortexed briefly to mix, incubated for 5 min at room temperature, centrifuged at 5000×*g* for 10 min to pellet the cells and stored at −80 °C until processing.

Total mRNA was extracted using the illustra RNAspin Mini Kit (GE Healthcare Life Sciences). The eluted total RNA was subjected to an additional DNaseI digestion step to remove genomic DNA using the TURBO DNA-*free* Kit (Life Technologies). Concentrations were measured using Nanodrop 2000 (Thermo Scientific). Next, the cDNA was synthesized using the QuantiTect Reverse Transcription Kit (Qiagen), ensuring that equal amounts of RNA were added to every reaction for normalization across samples. Protocols were followed as provided by the respective kits. Quantitative PCR was performed using the ABI 7300 Real Time PCR System (Applied Biosystems), and the 2X Brilliant II SYBR qPCR High ROX Master Mix (Agilent Technologies). Reactions contained 2 μL of cDNA from the corresponding RNA isolation, as well as appropriate primers and the master mix quantities as described by the protocols provided with the kit to give a total reaction volume of 25 μL. Amplification was carried out using the following program: initial incubation at 95 °C for 10 min, followed by 40 cycles of 95 °C for 30 s and 60 °C for 1 min. Threshold cycle values were set by the software and the C_T values for each respective sample were obtained and used to calculate fold-differences in *pfkA* transcript levels compared to IB2275.

Quantification of extracellular metabolites. Glucose, MI, acetate and glucaric acid levels were quantified by high performance liquid chromatography (HPLC) on an Agilent 1100 or 1200 series instrument (Santa Clara, CA) with an Aminex HPX-87H column (300 mm by 7.8 mm; Bio-Rad Laboratories, Hercules, CA). Sulfuric acid (5 mM) at a flow rate of 0.6 mL/min (isocratic) was used as the mobile phase. Compounds were quantified from 10 μL sample injections using a refractive index detector. Column and refractive index detector temperatures were held at 55 °C.

Shikimate was quantified with a ZORBAX SB-Aq column (4.6 mm × 150 mm × 3.5 μm). The HPLC was run with a mixture of solution A (20% methanol) and solution B (25 mM Ammonium formate, pH 2.5) as eluent at a flowrate of 0.6 mL/min. The following gradient was used: at 0–2 min, 2% solution A and 98% solution B; by 17 min, 10% solution A and 90% solution B; by 18 min, 100% solution A and 0% solution B; at 18–19 min, 100% solution A and 0% solution B; by 20 min, 2% solution A and 98% solution B; at 20–22 min, 2% solution A and 98% solution B. Compounds were quantified with 10 μL injections using diode-array detection.

Statistics. All error bars are reported as s.d. of replicates. The number of replicates is provided in the corresponding figure caption. Where relevant, two-tailed *t*-tests are used to demonstrate differences in values.

41. Shong, J., Huang, Y.-M., Bystroff, C. & Collins, C.H. Directed evolution of the quorum-sensing regulator EsaR for increased signal sensitivity. *ACS Chem. Biol.* **8**, 789–795 (2013).
42. St-Pierre, F. *et al.* One-step cloning and chromosomal integration of DNA. *ACS Synth. Biol.* **2**, 537–541 (2013).
43. Kuhlman, T.E. & Cox, E.C. Site-specific chromosomal integration of large synthetic constructs. *Nucleic Acids Res.* **38**, e92 (2010).
44. Shong, J. & Collins, C.H. Engineering the esaR promoter for tunable quorum sensing-dependent gene expression. *ACS Synth. Biol.* **2**, 568–575 (2013).
45. Baba, T. *et al.* Construction of *Escherichia coli* K-12 in-frame, single-gene knockout mutants: the Keio collection. *Mol. Syst. Biol.* **2**, 2006.0008 (2006).
46. Reisch, C.R. & Prather, K.L.J. The no-SCAR (Scarless Cas9 Assisted Recombineering) system for genome editing in *Escherichia coli*. *Sci. Rep.* **5**, 15096 (2015).
47. Salis, H.M. The ribosome binding site calculator. *Methods Enzymol.* **498**, 19–42 (2011).

doi:10.1038/nbt.3796